Title

Evaluation of electrospray differential mobility analysis for virus particle analysis: Potential applications for biomanufacturing

Journal

Journal of Virological Methods, 178(1-2)

ISSN

0166-0934

Authors

Guha, Suvajyoti
Pease, Leonard F
Brorson, Kurt A
et al.

Publication Date

2011-12-01

DOI

10.1016/j.jviromet.2011.09.012

Peer reviewed

Since January 2020 Elsevier has created a COVID-19 resource centre with free information in English and Mandarin on the novel coronavirus COVID-19. The COVID-19 resource centre is hosted on Elsevier Connect, the company's public news and information website.

Journal of Virological Methods 178 (2011) 201–208

Contents lists available at SciVerse ScienceDirect

Journal of Virological Methods

journal homepage: www.elsevier.com/locate/jviromet

Evaluation of electrospray differential mobility analysis for virus particle analysis: Potential applications for biomanufacturing

Suvajyoti Guha[a,b], Leonard F. Pease III[a,c], Kurt A. Brorson[d], Michael J. Tarlov[a], Michael R. Zachariah[a,b,*]

[a] National Institute of Standards and Technology (NIST), Gaithersburg, MD 20899, United States
[b] Departments of Mechanical Engineering, Chemistry and Biochemistry, The University of Maryland, College Park, MD 20742, United States
[c] Departments of Chemical Engineering, Pharmaceutics & Pharmaceutical Chemistry, and Internal Medicine, The University of Utah, Salt Lake City, UT 84112, United States
[d] Center for Drug Evaluation and Research (CDER), Food and Drug Administration, Silver Spring, MD 20903, United States

Article history:
Received 26 May 2011
Received in revised form
12 September 2011
Accepted 15 September 2011
Available online 22 September 2011

Keywords:
Electrospray
Differential mobility analyzer
Virus
ICH Q2
Gas phase electrophoretic molecular mobility analysis (GEMMA)

A B S T R A C T

The technique of electrospray differential mobility analysis (ES-DMA) was examined as a potential potency assay for routine virus particle analysis in biomanufacturing environments (e.g., evaluation of vaccines and gene delivery products for lot release) in the context of the International Committee of Harmonisation (ICH) Q2 guidelines. ES-DMA is a rapid particle sizing method capable of characterizing certain aspects of the structure (such as capsid proteins) and obtaining complete size distributions of viruses and virus-like particles. It was shown that ES-DMA can distinguish intact virus particles from degraded particles and measure the concentration of virus particles when calibrated with nanoparticles of known concentration. The technique has a measurement uncertainty of ≈20%, is linear over nearly 3 orders of magnitude, and has a lower limit of detection of $\approx 10^9$ particles/mL. This quantitative assay was demonstrated for non-enveloped viruses. It is expected that ES-DMA will be a useful method for applications involving production and quality control of vaccines and gene therapy vectors for human use.

1. Introduction

Evaluating the titer (concentration) of viral products as part of a lot release protocol is a key quality control step essential to ensuring their efficacy and safety (ICH Expert Working Group, 2005). Although the specific tests comprising the lot release protocol are prescribed individually for each product as appropriate for each case, the assays and instruments used to evaluate the identity, composition and potency of viral products must meet standards established by the International Committee on Harmonisation (ICH) (ICH Expert Working Group, 2005). Specifically, "ICH Q2 Validation of Analytical Procedures: Text and Methodology" indicates that a quantitative assay must be evaluated based on seven criterion, namely; specificity, linearity, range, accuracy, precision, robustness, and system suitability testing (ICH Expert Working Group, 2005).

Common tests used to identify the concentration and composition of viruses includes transmission electron microscopy (TEM), scanning electron microscope (SEM), analytical ultracentrifugation and dynamic light scattering. Although each of these methods possesses particular strengths for evaluating viral products, they all have disadvantages. For example, while TEM provides high resolution images, it is expensive, relatively slow, and artifacts can be introduced from electron beam damage, sample preparation, and biases in particle selection for quantitative analysis. In contrast, dynamic light scattering is relatively fast and can analyze the sample *in situ*; however, it cannot accurately differentiate viral particles differing by less than 10 nm in diameter or easily quantify virus particles either (Filipe et al., 2010). Resolving particles that are close in size is an important criteria, as viral degradation often leads to mixtures of intact and partially degraded viruses that can differ in diameter by 10 nm or less.

The objective of this article was to present ES-DMA (Fig. 1) as a potential method for analysis in biomanufacturing environments (e.g., evaluation of gene therapy produces, vaccines for routine lot release, etc.) where relatively concentrated solutions of particles 20–200 nm in size are measured. The advantages of ES-DMA for characterizing vaccines include its ability to provide a direct readout of particle size distributions, to measure rapidly statistically significant populations of nanoparticles, and to detect changes in nanoparticle diameter as small as 0.3 nm, far below the size of the smallest viruses (Tsai et al., 2008, 2009). In addition, viruses can be identified based on particle size, thereby ruling out contaminating adventitious agents unless they are of the same size. Size

* Corresponding author at: 2125 Glenn L. Martin Hall, Building 088, University of Maryland, College Park, MD 20742 United States. Tel.: +1 301 405 4311; fax: +1 301 314 9477.
E-mail address: mrz@umd.edu (M.R. Zachariah).

0166-0934/$ – see front matter © 2011 Published by Elsevier B.V.
doi:10.1016/j.jviromet.2011.09.012

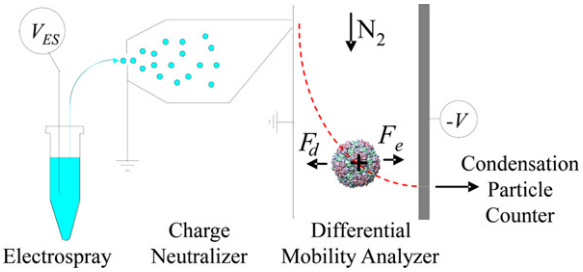

Fig. 1. ES-DMA system consisting of an electrospray-charge neutralizer to produce aerosolized, singly charged virus and protein particles, a differential mobility analyzer to separate them by their charge-to-size ratio (because electrical and drag forces act on them, F_e and F_d, respectively), and a condensation particle counter to enumerate the size-selected viruses or proteins.

measurement by ES-DMA also does not rely on host-specific infectivity or species specific qPCR primers.

Over the last decade, ES-DMA has been applied broadly to characterize phage and virus-like particles. For example, a number of studies measured the size of both large and small viruses (Bacher et al., 2001; Bothner and Siuzdak, 2004; Wick et al., 2005; Hogan et al., 2006; Thomas et al., 2004; Cole et al., 2009; Kaddis et al., 2007; Laschober et al., 2008; Pease et al., 2009; Wick et al., 2007). Using ES-DMA size distributions Pease et al. (2011) determined the symmetry and number of proteins per capsid for PR772 (Family *Tectiviridae*, Genus *Tectivirus*), a biosafety level 1 (BSL1) simulant of adenovirus. Lute et al. (2008) and Wick et al. (2007) extended ES-DMA analyses to viruses of particular interest to biomanufacturers and filter firms by characterizing the size distributions of murine minute virus (Family *Parvoviridae*, parvovirus) and the BSL1 models, PP7 (Family *Leviviridae*, Genus *Levivirus*) and ϕX174 (Family *Microvaridae*, Genus *Microvirus*) (Wick et al., 2007) used in virus filtration studies (Lute et al., 2008) and in the Parenteral Drug Association's (PDA) new nomenclature standards for small and large virus retentive filters. Wick et al. (2005) demonstrated that ES-DMA is sufficiently gentle to enveloped viruses such as alphavirus (Family *Togaviridae*) although there was some loss of structure in murine hepatitis virus (Family *Coronaviridae,* Genus *Coronavirus*), and sendai rodent virus (Family *Paramyxoviridae*, Genus *Respirovirus*). Using a novel recombinant virus-like particle as a test article, Pease et al. (2009) recently compared ES-DMA size distributions to those of TEM and asymmetric flow field-flow fractionation and found good agreement among the techniques for particle quantitation. Furthermore, it was shown that icosahedra viruses remain infectious following electrospray (Hogan et al., 2006; Siuzdak et al., 1996; Thomas et al., 2004), though long tubular viruses appear to lose structural integrity and infectivity in the electrospray. Overall, this technique has the potential to analyze many types of viruses.

ES-DMA operates at atmospheric conditions thereby introducing a drag force on the charged particle. Thus, unlike mass spectrometry which separates particles on the basis of their mass-to-charge ratio, the DMA separation is based on charge-to-size ratio. In the size regime of relevance to these studies, the DMA "size" metric of separation is the projected areas orthogonal to the principle axes of the particles, which for a spherical particle is simply the area of a circle of the same radius (Pease et al., 2010). Like mass-spectrometry, electrospray is used for sample delivery; however, in ES-DMA, droplets are immediately neutralized by passage through a radioactive source (Po-210) positioned at the exit of the electrospray. These droplets, some of which contain particles of interest, dry as they pass through the neutralizer, leaving 5–20% of the dry, aerosolized particles with a single positive charge (Weidensohler, 1988). Scanning through a range of charge-to-size ratios gives a detailed size distribution for the virus containing solution. ES-DMA can be used to size particles ranging from three to hundreds of nanometers in diameter and differentiate spherically equivalent sizes as small as 0.3 nm at its highest reported resolution (Tsai et al., 2008, 2009).

In the following sections, ES-DMA is evaluated based on ICH Q2 principles after the preparation protocols for the different materials and the operating conditions for ES-DMA are presented.

2. Materials and methods

2.1. Test article preparation

Phage PP7 and its host *Pseudomonas aeruginosa* were obtained from the ATCC (Manassas, VA; accession numbers 15692-B4 and 15692). Coliphage PR772 and host *E. coli* strain K-12 J-53-1 were obtained from the Félix d'Hérelle Reference Center for Bacterial Viruses (Université Laval, Québec, Canada). These bacteriophage models were used instead of actual mammalian viruses because they can be easily grown to high titer and can be prepared and studied under BSL1 conditions. Stocks were prepared by CsCl gradient ultracentrifugation methods, and live intact phages were enumerated by plaque assays using their respective hosts, as described elsewhere (Lute et al., 2004, 2007). The phages were then dialyzed into 2.0 mmol/L ammonium acetate, pH 7.4, in preparation for the electrospray. Studies showed that short term storage (≈months) in this buffer system did not significantly impact phage infectivity (results not shown). For PR772 the dialyzed sample at an initial concentration of 1.5×10^{12} plaque forming units/mL (pfu/mL) was diluted to prepare a serial dilution of 4×, 10×, 50×, 500× and 5000× and have been henceforth referred to as PR772a, PR772b, PR772c, PR772d and PR772e, respectively. For PP7, dialysis a parent stock resulted in an initial concentration of 2.5×10^{13} pfu/mL. Then a fifty times dilution from the above stock was prepared from which serial dilutions of 2×, 5×, 50×, 500× and 1000× were prepared and have been henceforth referred to as PP7a, PP7b, PP7c, PP7d and PP7e, respectively.

Analysis in this article was limited to viral particles in solutions in which nonvolatile salts, surfactants, or other materials present in formulation buffers had largely been removed. The presence of these species were found to cause clogging of electrospray capillaries, destabilizing the electrospray and resulting in noisy size distributions. Other factors that affect the stability of the electrospray include capillary diameter, ionic strength outside of a specific conductivity window, and protein or buffer species that affect the surface tension.

To create partially degraded test samples, dialyzed PR772 and PP7 samples were placed in 1.5 mL protein low binding centrifuge vials (Eppendorf North, Westbury, NY, USA, #022431081) and heated using a BLOK heater (Labline Instruments Inc, Melrose Park, IL, USA, #2003) to temperatures from 50 °C to 80 °C. The samples were heated within 2 min to the desired temperature, and maintained within ±1.0 °C as measured by a type K thermocouple (Omega, Stamford, Connecticut, USA) inserted directly into sample vials via holes punctured through their caps. After 30 min the samples were removed from the BLOK heater. Control samples for comparison were held at ambient temperature (25 °C) for 30 min.

For infectivity assays, dilutions of the virus stocks and heat treated samples were prepared and added to mid-log-phase host and liquefied top agar, which was spread over tryptic soy agar plates.

2.2. Buffer preparation

Electrospray buffer was prepared by adding 0.77 g of ammonium acetate (Sigma–Aldrich, St. Louis, MO, #631-61-8) to 0.5 L of deionized water (18 MΩ/cm, Barnestead nanopure UV system) and

adjusting to the desired pH using ammonium hydroxide (Baker, Phillipsburg, NJ, #9721-01).

2.3. Gold nanoparticles preparation

For quantitative number concentration calibration of the ES-DMA, gold nanoparticle reference standards were used. One milliliter aliquots of as received 20 nm and 60 nm Ted Pella gold initially at particle concentrations of 7.0×10^{11} particles/mL and 2.6×10^{10} particles/mL were centrifuged for 20 min and 10 min, respectively, at 13,200 rpm which were subsequently concentrated to prepare stock concentrations of 3.4×10^{12} particles/mL and 2.6×10^{11} particles/mL for 20 nm and 60 nm samples, respectively. Two different sizes were selected because the sensitivity of ES-DMA depends on size, with sensitivity increasing with particle size. Serial dilutions of 2, 4, 8, 16, 32, and 64 times for the 20 nm and 2, 4, 8, and 16 times for 60 nm were then prepared from this stock.

2.4. ES-DMA operation and data analysis

Centrifuge vials containing the samples for ES-DMA were inserted into the pressure chamber of an electrospray aerosol generator (TSI Inc., USA, #3480). A pressure of 3.7 psi (26 kPa) in the head space drove flow (≈66 nL/min) through a 25 μm inner diameter capillary at the exit of which a voltage was tuned to form the meniscus into a conical shape Taylor cone. The current observed in the electrospray typically varied from 290 nA to 340 nA. A stream of gas, consisting of 1.1 L/min of air, flowed coaxially with the capillary to carry the highly charged droplets into a bipolar charge neutralizer (Po-210) placed at the exit of the ES, to produce a stream of particles with a known charge distribution (Weidensohler, 1988; Kim et al., 2005). These charged aerosolized virus particles were then passed into the differential mobility analyzer. The DMA (TSI Inc., USA, #3080) was operated with a sheath flow of 30 L/min for PP7 or 10 L/min for PR772. Because the trajectory of the virus particles is controlled by balancing the electrical and drag forces acting on them, only those with a selected charge-to-size ratio, for the applied electric field chosen, passed into the collection slit for counting. By stepping through different electric fields, a size distribution was obtained, in increments of 0.2 nm (Wang and Flagan, 1990). The size reported in this article is the spherically equivalent size obtained using Stokes drag law corrected with the velocity slip correction (Hinds, 1999).

Particles (viruses and capsid proteins) exiting the DMA were counted using a condensation particle counter (CPC) (TSI Inc., USA, #3025A) (Kesten et al., 1991). Flow into the CPC consisted of 1.0 L/min exiting the DMA supplemented by 0.5 L/min of ambient air filtered through a HEPA filter to allow the CPC to operate in its high flow mode. Within the CPC, particles passed through a saturated butanol environment and grew by condensation into droplets several micrometers in size, which were counted individually by light scattering.

The raw ES-DMA distributions present counts or number density of positively charged particles versus the spherically equivalent mobility diameter. The positively charged virus particles measured represented only a fraction of all of the viruses emerging from the electrospray. The total gas phase particle count for each size was obtained by dividing the number of positively charged viruses by the fraction of positively charged viruses, which depends primarily on the particle size (Weidensohler, 1988). As described in a previous publication, an "overlap correction" was also applied to prevent double counting of essentially the same particles (Pease et al., 2010).

Gold nanoparticles (Ted Pella) prepared in ammonium acetate buffer (Tsai et al., 2008) or 60 nm polystyrene latex particles (NIST SRM® 1963) were used as system suitability standards to confirm operation of the instrumentation (Lall et al., 2009).

2.5. Gold calibration approach

In order to correlate gas phase concentration with liquid phase, Cole et al. (2009) used known concentrations of gold nanoparticles to calibrate the ES-DMA system to determine the concentration of virus particles. The ratio of particles in solution and signal intensity from the DMA gave the response function of the DMA system. The response function was then used to obtain virus concentration in solution. Virus concentration values determined this way were found to be in good agreement with amino acid analysis (Cole et al., 2009). A similar protocol was used in this article to determine concentrations of PP7 and PR772.

Two different gold nanoparticles sizes of known concentrations were selected; nominally 20 nm and 60 nm, to approximate particles close in size to PP7 and PR772. Serial dilutions of 20 nm citrate stabilized Ted Pella gold nanoparticles, as mentioned in Section 2.3, were created to obtain a response function for the ES-DMA of $6.21 \times 10^{-8} \pm 4.6 \times 10^{-9}$ (particles/cm^3)/(particles/mL) for PP7 where the response function is defined as the ratio of the concentration measured in gas phase using ES-DMA and the actual particle concentration in solution. Similarly using 60 nm particles, a response function of $9.15 \times 10^{-8} \pm 8.0 \times 10^{-9}$ (particles/cm^3)/(particles/mL) for PR772 was obtained. The difference in response functions for PP7 and PR772 was likely due to different ES-DMA settings and operational parameters used (e.g., particle size dependent diffusional losses).

2.6. TEM characterization

TEM analysis employed a standard negative staining procedure performed by JFE Enterprise (Brookeville, MD). Briefly, a drop of 0.01% of BSA was placed on a formvar/carbon coated grid and wicked off with filter paper. Then 2.0 μL of the virus was applied on the coated grid and allowed to air-dry. The grid was washed with distilled water twice and air dried. Subsequently, 10 μL of 1.0% uranyl acetate was placed on the grid, allowed to stain for 30 s, wicked off and then allowed to air dry again before TEM imaging.

3. Results

Like any assay, ICH Q2 should be used to validate ES-DMA for any particular application, e.g., testing particle size distributions of vaccines or gene therapy vectors. According to ICH Q2, "the objective of validation of an analytical procedure is to demonstrate that it is suitable for its intended purpose." This guidance recommends evaluation of a quantitative assay along seven lines of inquiry; namely specificity, linearity, range, accuracy, precision, robustness, system suitability, limit of detection (LoD) and limit of quantitation (LoQ). In the remainder of this article, the phages were considered as though they were the models for industrially relevant virus preparations of interest and the performance of ES-DMA was evaluated as a quantitative assay relative to ICH Q2 criteria to measure the viral analyte present in the sample.

3.1. Specificity

Demonstration of specificity confirms the ability of an assay to distinguish the species of interest within a sample from extraneous material or closely related species such as contaminating adventitious viruses. ICH Q2 states that specificity must "assess unequivocally the analyte in the presence of

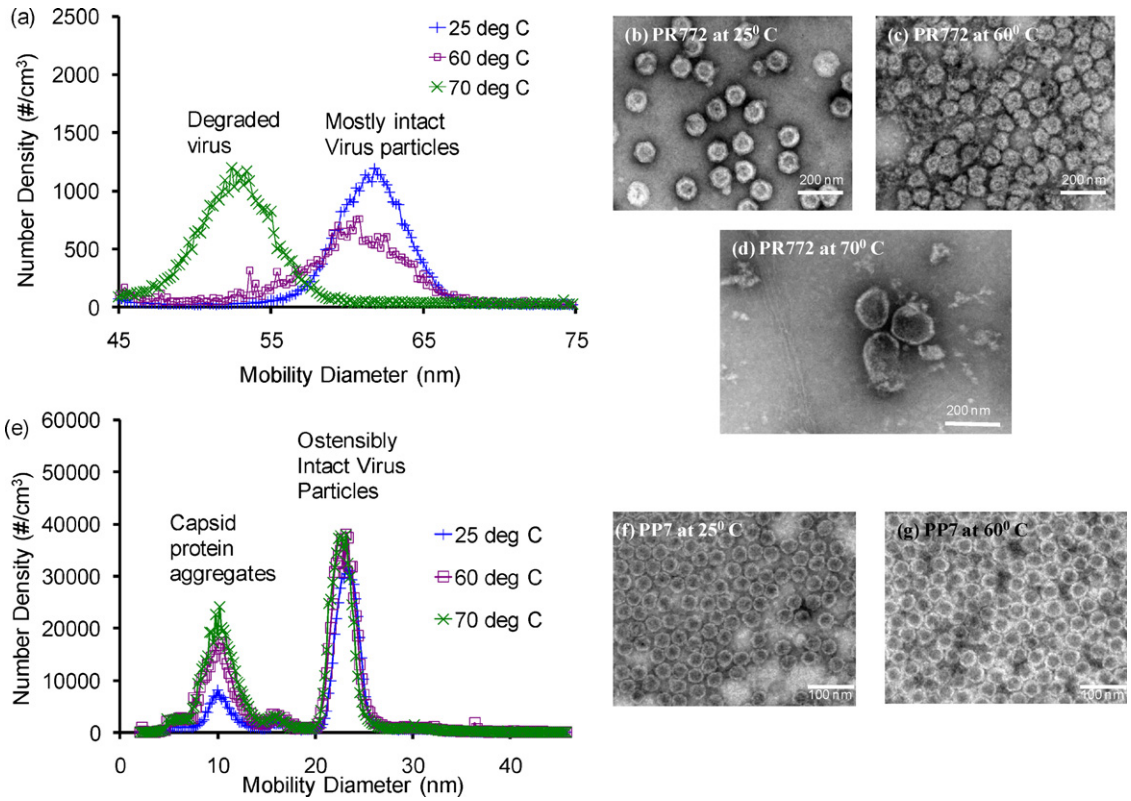

Fig. 2. (a) ES-DMA size distributions for PR772 and TEM images of PR772 (b) untreated and heated for 30 min to (c) 60 °C and (d) 70 °C. (e) ES-DMA size distributions for PP7 and TEM images of PP7 (f) untreated and (g) heated for 30 min to 60 °C.

components. . .including impurities, degradants, matrix, etc." (ICH Expert Working Group, 2005).

ES-DMA can differentiate intact virus particles from impurities associated with degradation products, e.g., capsids that are partially or completely degraded. To model such impurities, virus particles were thermally degraded for 30 min at temperatures up to 70 °C, and ES-DMA size distributions and TEM images were obtained for PR772 and PP7 before and after thermal treatment (Fig. 2). ES-DMA size distributions for PR772 (Fig. 2a) showed two peaks corresponding to degraded viruses (≈50 nm) at 70 °C and intact viruses (≈60 nm) at ambient temperature and 60 °C. The full size distribution (Fig. S1) also included a third peak at ≈8.0 nm which was assigned to P3 trimers (Lute et al., 2004) based on Bacher et al's (2001) molecular weight correlation. Larger structures that were likely aggregates of the capsid proteins also appeared between 10 nm and 20 nm and increased in intensity with increasing incubation temperatures (Fig. S1). The specificity of ES-DMA was confirmed by comparing ES-DMA size distributions to TEM micrographs. The TEM micrographs showed a similar trend of intact particles at ambient conditions, partially degraded particles at 60 °C and then completely degraded particles at 70 °C with predominantly intact virus particles (Fig. 2b) and degraded particles (Fig. 2c and d). Some particles of size 100–200 nm were seen (Fig. 2d) but possibly were below the limit of detection of the ES-DMA, for only a few were found in the TEM micrographs.

The ES-DMA size distribution of PP7 (Fig. 2e) showed putatively intact virus particles (≈23 nm) and degraded capsid proteins or their aggregates at smaller sizes (≈10 nm) that increased in concentration with incubation temperature. Similarly, the TEM micrographs, at ambient conditions showed no difference from sample heated at 60 °C (Fig. 2f); however, in contrast to ES-DMA data, there was little evidence of degraded capsids proteins. Nevertheless, the agreement confirmed ES-DMA's ability to identify specifically intact and partially degraded capsids or aggregates of capsid proteins.

3.2. Precision, linearity and accuracy

The linearity, accuracy and precision of ES-DMA for measuring the concentration of virus particles were determined. Five different dilutions each of PP7 and PR772 were prepared and their

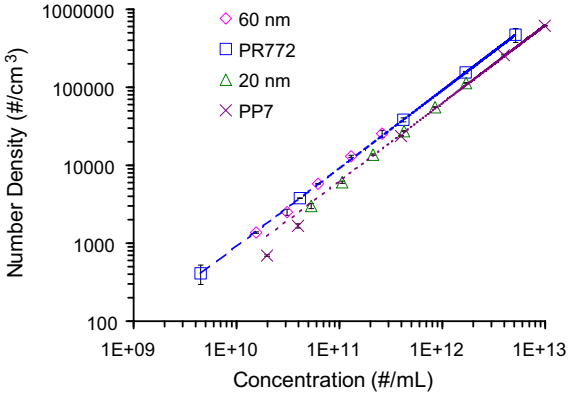

Fig. 3. ES-DMA aerosol number density, N, versus solution concentration, C, for PP7 and PR772. The linear fits were $\log_{10}(N) = 0.9774 \log_{10}(C) - 5.6782$ with $R^2 = 0.9995$(denoted by long blue dash) for PR772 and $\log_{10}(N) = 1.09 \log_{10}(C) - 6.1662$ (denoted by short purple dash) with $R^2 = 0.9993$ for PP7. The linear fits for 60 nm and 20 nm Au were $\log_{10}(N) = 0.9425 \log_{10}(C) + 7.2533$ with $R^2 = 0.9989$ and $\log_{10}(N) = 0.9439 \log_{10}(C) + 7.4424$ with $R^2 = 0.9996$, respectively. The error bars, if not visually apparent, were smaller than the symbols and were from samples run in triplicate. The long (blue) and short (purple) dashed lines guide the eyes. (For interpretation of the references to color in this figure legend, the reader is referred to the web version of this article.)

concentrations were determined by a plaque-based assay and ES-DMA. For virus particle concentration measurement, the PP7 peak included counts from 21.0 nm through 26.8 nm and the PR772 peak included counts from 55.0 nm to 67.8 nm. The mean mobility diameter of PR772 and PP7 were determined to be 62.1 nm ± 0.4 nm and 23.8 ± 0.3 nm respectively for size distributions obtained in triplicate. All linearity studies were performed using the same capillary to rule out any differences arising from different capillaries. ES-DMA gas phase number density as a function of solution concentration of PR772 and PP7 was plotted over a solution concentration range from 4.48×10^9 particles/mL to 5.15×10^{12} particles/mL and 1.12×10^{10} particles/mL to 9.9×10^{12} particles/mL for PR772 and PP7, respectively (Fig. 3). The values of the exponents for PR772 and PP7 were determined to be 0.9974 and 1.09, respectively, indicating linearity (Fig. 3, caption). R^2 values in excess of 0.99 for both the cases indicated that the fit was good.

ES-DMA characterizes two properties of particles: size and number concentration. The accuracy of ES-DMA for determination of size were established for spherical and nearly spherical particles elsewhere (Tsai et al., 2009; Mulholland et al., 2006). Accuracy of ES-DMA for determination of concentration can be established usually by comparing results with another orthogonal technique although methods are not always directly comparable as given below.

To relate ES-DMA counts to concentration of virus particles in solution, ES-DMA was calibrated by analyzing gold nanoparticles of known concentration as was discussed in Section 2.5. The absolute liquid phase virus concentration was also determined by ES-DMA (column 4, Table 1). Particle measurements were 11-15 fold (PR772) and 22-42 fold (PP7) greater than their infectivity (Table 1), showing that these preparations were 2–10% infectious in agreement with previous results (Cole et al., 2009).

In order to compare the inter-day precision with intra-day precision, samples PR772c and PP7b were measured repeatedly on an individual day to determine the repeatability and across several days to measure the intermediate precision. The data was found to fall within relatively narrow bands (Table 2). It was observed that for both PP7 and PR772 the intra-day variations were smaller than the inter-day variation, as is typical for precision studies. The larger inter-day variation was expected because over this time period, the ES-DMA system was shut down (which consists of switching off the ES, sheath flow and the CPC) and restarted which may have caused modest differences in flow rates or may have affected the performance of the DMA or the CPC. In addition, the effect of changing capillaries was also studied, an issue addressed in greater detail in Section 3.5. It should be pointed out that the gas phase repeatability counts obtained with the ES-DMA for PP7b in Table 1 and Table 2 are different as they were obtained on different days.

3.3. Detection and quantitation limits

The limits of detection and quantitation were determined using the signal-to-noise method indicated in ICH Q2 Sections 6.2 and 7.2. First, the CPC baseline was determined by electrospraying ammonium acetate buffer through a capillary and by obtaining size distributions of this control buffer from 2 nm to 45 nm for PP7 or 2 nm to 75 nm for PR772. Then, the baseline where PP7 (21 nm to 26.8 nm) and PR772 (55 nm to 68 nm) would appear were summed to obtain the limit of detection for these viruses, respectively. This was repeated in triplicate and the uncertainty in CPC (aerosol phase) counts in the baseline was determined to be 45 particles/cc ± 14 particles/cc and 7 particles/cc ± 2 particles/cc for the measured size range of PP7 and PR772, respectively (data not shown). The product of the measured uncertainty with the average response functions of 20 nm and 60 nm Au nanoparticles gives a measure of the liquid phase noise level for PP7 and PR772, respectively. Further, since ICH Q2 specifications for LoD require a signal-to-noise ratio of 3:1, the liquid phase noise was multiplied by three to obtain LoDs of 7.3×10^8 particles/mL for PP7 and 2.3×10^8 particles/mL for PR772, respectively. Expressing these values as plaque assay LoDs (pfu/ml) yielded 2.3×10^7 pfu/mL (assuming particle:infectivity ratio of ≈32) and 1.7×10^7 pfu/mL (assuming particle:infectivity ratio ≈14) for PP7 and PR772, respectively. These values were distinctly higher than the LoD of approximately 10^6 infectious virus/mL determined by Hogan et al. (2006) for bacteriophage viruses although they did not report a baseline uncertainty.

The limit of quantitation (LoQ) was determined using a similar signal-to-noise method. For the LoQ, all steps were similar to that described for LoD except the last one where the liquid phase noise in the above data was multiplied by ten instead of three as per ICHQ2, resulting in LoQs of 2.5×10^9 particles/mL and 7.5×10^8 particles/mL for PP7 and PR772, respectively. Expressing the concentration in terms of pfu/mL, the LoQ were determined to be 7.7×10^7 pfu/mL and 5.6×10^7 pfu/mL for PP7 and PR772, respectively.

3.4. Range

ICH Q2 also requires a determination of the dynamic range of the instrument. The LoQ as specified above defined the lower end of the range. The instrument has an upper limit of 10^6 particles/cm^3 (in the aerosol phase), but any highly concentrated solution can always be diluted to reduce the concentration to the linear region of the instrument. Thus, the upper range can be defined by the highest particle titer in a test particle.

3.5. Robustness

For ES-DMA the primary factors that influence size and concentrations are ambient temperature variations; fluctuations of the gas flow in the electrospray, DMA and CPC; performance of the neutralizer; and variation in capillaries. ICH Q2 calls for investigation of such parameters under the rubric of robustness. Ambient temperature variations may influence the gas flows in the ES, the DMA as well as the CPC. The performance of the DMA depends on the relative rates of a carrier gas in the DMA and the analyte carrier gas (Tsai et al., 2008, 2009) that arrives from the ES. Any changes in these flows can cause apparent changes in size and concentration of the particles of interest. Additionally, the flow rates may also vary slightly over time even without temperature changes. Each change may cause variation in counts and size obtained by ES-DMA assay over several hours on the same day or over several days as has been addressed under the rubric of "repeatability" and "intermediate precision" (Section 3.2). Further, the neutralizing source used for charge reduction (Po-210) has a half-life of 138 days, and should be operated under conditions of excess alpha radiation to neutralize the ionized particles. Extended operation of the same Po-201 source past one year can lead to a degraded charging efficiency. Capillaries in the electrospray often need to be changed, because of clogging from either very large impurities (micron sized) in the solution, or from deposition of particles on the electrospray tip with time, both of which affects ES-DMA concentration measurements. To study this variation, the PP7 and PR772, size distributions were obtained using three different capillaries on the same day. For PP7 and PR772 the mean diameters obtained were 23.7 nm ± 0.1 nm and 61.9 nm ± 0.3 nm in conjunction with linearity studies, which implied that changing the capillaries did not affect the size. However, concentrations determined by the ES-DMA were found to vary with change of capillaries (last two rows, Table 2). These variations were found to be comparable to the intermediate precision, i.e.,

Table 1
ES-DMA as compared to plaque assay.

	Plaque assay derived concentration (pfu/mL)	ES-DMA gas-phase particle counts (particles/cm^3)[a]	ES-DMA (concentration in solution particles/mL)	Ratio (ES-DMA particles/mL)/(pfu/mL)
PR772a	3.75×10^{11}	471700 ± 96400	5.15×10^{12}	14
PR772b	1.5×10^{11}	154400 ± 5100	1.69×10^{12}	11
PR772c	3.00×10^{10}	38300 ± 2300	4.18×10^{11}	14
PR772d	3.00×10^{9}	3800 ± 20	4.13×10^{10}	14
PR772e	3.00×10^{8}	400 ± 110	4.48×10^{9}	15
PP7a	2.50×10^{11}	614800 ± 7300	9.90×10^{12}	40
PP7b	1.00×10^{11}	258500 ± 6600	4.16×10^{12}	42
PP7c	1.00×10^{10}	23700 ± 330	3.81×10^{11}	38
PP7d	1.00×10^{9}	1700 ± 110	2.69×10^{10}	27
PP7e	5.00×10^{8}	700 ± 20	1.12×10^{10}	22

[a] Samples run at least in duplicate.

Table 2
Repeatability, intermediate precision and capillary variation statistics for ES-DMA.

	Average (particles/cc)	Standard deviation (particles/cc)	Coefficient of variation	Confidence interval[*,**] (%)
Repeatability PR772c	38,300	2300	0.060	5.7
Repeatability PP7b	2,69,300	13,500	0.050	4.8
Intermediate precision PR772c	33,270	6950	0.209	19.8
Intermediate precision PP7b	2,65,200	17,400	0.066	6.2
Capillary variation PR772c	31,600	3200	0.101	9.6
Capillary variation PP7b	2,71,140	34,750	0.128	12.2

[*] http://www.itl.nist.gov/div898/handbook/prc/section1/prc14.htm.
[**] Calculations done at 90% confidence level for samples run in triplicate.

changing capillaries on one day had as much effect as did other day-to-day factors (such as flow and temperature fluctuations).

4. Discussion

Manufacturers routinely characterize vaccines and gene delivery products when releasing lots or performing stability studies. Determining the purity of final product and assessing concentration at various stages of product processing are of paramount interest. While techniques such as TEM and dynamic light scattering can be used, drawbacks include long analysis times (TEM), skewing of size for multimodal distributions (dynamic light scattering) and dependence of results on infectivity (plaque assays). Other characterization techniques such as antigen detection and nucleic acid detection and amplification are also popular but they either require specific antibodies or high concentrations (EPIDI, 2009). Also, plaque-forming assays cannot distinguish between a single virus or an aggregate of several viruses which could potentially disassociate upon administration to humans and cause an over dose Malloy (2010). MS is gaining popularity for characterization Ding et al. (2007), but has been primarily applied to analysis of proteins of viruses (Davison and Davison, 1995; Krokhin et al., 2003; Yao et al., 2002) and rarely for entire capsids because of their large sizes (>1 MDa) resulting in high m/z ratios (Tito et al., 2000). Also, MS spectra can be complex and size distributions can be difficult to interpret because of multiple charging of particles (Tito et al., 2000).

In contrast, ES-DMA is a near real time method that operates at atmospheric pressure, and can resolve the whole size distribution from capsid proteins to the whole virus as has been demonstrated in Section 3.1. ES-DMA can achieve this objective by correlating identity with size. Thomas et al. (2004) has shown that the components of mixtures of very similar sized viruses can be distinguished based on size by ES-DMA. For example, they differentiated MS2 from RYMV based on a 4.3 nm size difference. Even though a database correlating size with identity has not yet been assembled using ES-DMA yet, a broad range of viruses can be distinguished based on their distinct mobility diameters as discussed in Section 1.

It is possible that two or more viruses may overlap in size such as MS2 and PP7 or HRV and GD7, making positive identification and complete discrimination difficult despite the subnanometer resolution (Tsai et al., 2008) of ES-DMA. However, in the case of industrial virus production, risk mitigating factors, such as stock characterization and adventitious agent testing, lower the risk of cross contamination of the widely different viruses.

To make the ES-DMA conducive to biomanufacturing, ES-DMA was evaluated in the context of ICH Q2. The ratio of particles/mL to pfu/mL for a given virus remained approximately constant as a function of decreasing virus concentration (Table 1). This suggested that the ES-DMA behaved linearly for the concentration range examined. However, the ES-DMA and plaque assay data did not yield the same counts (Table 1), which implied that not all phage particles were infectious such that a direct comparison to infectivity data led to a 10–40 fold disparity in the measured values, a common observation in virology when comparing the infectivity assay to methods that physically count particles (Xu and Brorson, 2001; Brorson et al., 2002). This discrepancy between the plaque assay and the ES-DMA measured concentrations presumably involves several factors. ES-DMA is a physical measurement and counts all virus particles whether “live” or “dead”, while the plaque assay is infectivity count. To be infectious, a phage must land on the bacteria, penetrate the cell membrane, take over the cellular machinery, and then make copies of itself and finally lyse the bacteria. Each of these processes has an efficiency of less than 100% thus a 1:1 particle to infectivity ratio is rarely achieved for any type of virion. This also explains why the LoDs and LoQs had different limits depending on whether they were expressed with respect to particles/mL or pfu/mL. The plot of linearity (Fig. 3) showed that the data did not extrapolate through the origin, an observation consistent with that of Hogan et al. (2006) for MS2, T2, and T4 viruses suggesting possible variability in the plaque assay measurements or differences in depositional losses that arise from particles sticking to surfaces (with smaller particles showing a greater propensity

to stick because Brownian diffusion is more) which may be size and species specific. PP7 gas phase counts obtained with the ES-DMA started to deviate from linearity at concentrations below $\approx 10^{10}$ particles/mL perhaps because of imprecision at the LoD.

Concentration measurements with ES-DMA yielded an uncertainty of ≈10–20% (obtained by dividing the standard deviation with the average in Table 2), a value close to that reported in a previous study (Cole et al., 2009) and slightly lower than that of the virus infectivity assay, which has an uncertainty of up to ≈30% (unpublished observations). Additional advantages of ES-DMA compared to infectivity assays include faster analysis time (minutes compared to a day for plaque assay) and that the genetic sequence of the virus or a viral host is not required for analysis.

The LoD was found to be size dependent. As indicated by Hinds (1999), deposition losses due to particle diffusion increase strongly as the particle size decreases. These losses may occur in the neutralizer, DMA, entrance to the CPC, or all the intermediate connective tubings. Therefore, it is unsurprising that the LoD for PP7 would modestly exceed that for PR772 solely due to diffusion deposition losses.

In summary, as the first step towards potential industry use and acceptance, ES-DMA was examined as a tool for vaccine and gene therapy product characterization in the context of ICH Q2 guidelines. The ES-DMA characterizes both "alive" or inactivated viruses, potentially tracks their degradation, and can resolve aggregated species. Further ES-DMA is rapid, non-biologically based quantitative assay, effective for non-enveloped viruses, with a lower detection limit of $\approx 10^9$ particles/mL, and was found to meet the requirements set forth by ICH Q2.

Disclaimers

Reference to commercial equipment, supplies, or software neither implies its endorsement by the National Institute of Standards and Technology (NIST) and the Food and Drug Administration (FDA) nor necessarily implies it to be best suited for this purpose. Views expressed in this article reflect those of the authors and do not constitute official positions of the Food and Drug Administration or the US Government.

Acknowledgements

The authors acknowledge the Nanoscale Imaging Spectroscopy and Properties Lab (NISP) of Maryland Nanocenter, University of Maryland, College Park for use of their JEM 2100 LaB6 TEM. The authors also thank Scott Lute for assistance and training in preparing and enumerating the phages.

Appendix A. Supplementary data

Supplementary data associated with this article can be found, in the online version, at doi:10.1016/j.jviromet.2011.09.012.

References

Bacher, G., Szymanski, W.W., Kaufman, S.L., Zollner, P., Blaas, D., Allmaier, G., 2001. Charge-reduced nano electrospray ionization combined with differential mobility analysis of peptides, proteins, glycoproteins, noncovalent protein complexes and viruses. J. Mass. Spectrom. 36, 1038–1052.

Bothner, B., Siuzdak, G., 2004. Electrospray ionization of a whole virus: analyzing mass, structure, and viability. Chembiochem 5, 258–260.

Brorson, K., Xu, Y.A., Swann, P.G., Hamilton, E., Mustafa, M., de Wit, C., Norling, L.A., Stein, K.E., 2002. Evaluation of a quantitative product-enhanced reverse transcriptase assay to monitor retrovirus in mAb cell-culture. Biologicals 30, 15–26.

Wick, C.H., McCubbin, P.E., Birenzvige, A., 2005. Detection and Identification of Viruses Using the Integrated Virus Detection System (IVDS). Edgewood Chemical Biological Center, Aberdeen Proving Ground, MD.

Cole, K.D., Pease, L.F., Tsai, D.H., Singh, T., Lute, S., Brorson, K., Wang, L., 2009. Particle concentration measurement of virus samples using electrospray differential mobility analysis and quantitative amino analysis. J. Chromatogr. A 1216, 5715–5722.

Davison, A.J., Davison, M.D., 1995. Identification of structural proteins of channel catfish virus by mass-spectrometry. Virology 206, 1035–1043.

Ding, X., Becht, S., Gu, X., 2007. Vaccine Characterization Using Advanced Technology. BioPharm International. AOU, 16–22.

Expanded Programme on Immunization of the Department of Immunization VaB, 2009. Manual of rotavirus detection and characterization methods. WHO Document Production Services, Geneva, Switzerland.

Filipe, V., Hawe, A., Jiskoot, W., 2010. Critical evaluation of nanoparticle tracking analysis (NTA) by nanosight for the measurement of nanoparticles and protein aggregates. Pharm. Res. 27, 796–810.

Hinds, W.C., 1999. Aerosol Technology: Properties, Behavior and Measurement of Airborne Particles. John Wiley and Sons, New York, 48 p, 160 p.

Hogan, C.J., Kettleson, E.M., Ramaswami, B., Chen, D.R., Biswas, P., 2006. Charge reduced electrospray size spectrometry of mega- and gigadalton complexes: whole viruses and virus fragments. Anal. Chem. 78, 844–852.

ICH Expert Working Group, 2005. Validation of analytical procedures: text and methodology Q2(R1). In: International Conference on Harmonisation of Technical requirements for Registration of Pharmaceuticals for Human use.

Kaddis, C.S., Lomeli, S.H., Yin, S., Berhane, B., Apostol, M.I., Kickhoefer, V.A., Rome, L.H., Loo, J.A., 2007. Sizing large proteins and protein complexes by electrospray ionization mass spectrometry and ion mobility. J. Am. Soc. Mass Spectrom. 18, 1206–1216.

Kesten, J., Reineking, A., Porstendorfer, J., 1991. Calibration of aTsi-Model-3025 ultrafine condensation particle counter. Aerosol Sci. Technol. 15, 107–111.

Kim, S.H., Woo, K.S., Liu, B.Y.H., Zachariah, M.R., 2005. Method of measuring charge distribution of nanosized aerosols. J. Colloid Interface Sci. 282, 46–57.

Krokhin, O., Li, Y., Andonov, A., Feldmann, H., Flick, R., Jones, S., Stroeher, U., Bastien, N., Dasuri, K.V.N., Cheng, K.D., Simonsen, J.N., Perreault, H., Wilkins, J., Ens, W., Plummer, F., Standing, K.G., 2003. Mass spectrometric characterization of proteins from the SARS virus—a preliminary report. Mol. Cell. Proteomics 2, 346–356.

Lall, A.A., Ma, X.F., Guha, S., Mulholland, G.W., Zachariah, M.R., 2009. Online nanoparticle mass measurement by combined aerosol particle mass analyzer and differential mobility analyzer: comparison of theory and measurements. Aerosol Sci. Technol. 42, 1075–1083.

Laschober, C., Wruss, J., Blaas, D., Szymanski, W.W., Allmaier, G., 2008. Gas-phase electrophoretic molecular mobility analysis of size and stoichiometry of complexes of a common cold virus with antibody and soluble receptor molecules. Anal. Chem. 80, 2261–2264.

Lute, S., Aranha, H., Tremblay, D., Liang, D.H., Ackermann, H.W., Chu, B., Moineau, S., Brorson, K., 2004. Characterization of coliphage PR772 and evaluation of its use for virus filter performance testing. Appl. Environ. Microbiol. 70, 4864–4871.

Lute, S., Bailey, M., Combs, J., Sukumar, M., Brorson, K., 2007. Phage passage after extended processing in small-virus-retentive filters. Biotechnol. Appl. Biochem. 47, 141–151.

Lute, S., Riordan, W., Pease, L.F., Tsai, D.H., Levy, R., Haque, M., Martin, J., Moroe, I., Sato, T., Morgan, M., Krishnan, M., Campbell, J., Genest, P., Dolan, S., Tarrach, K., Meyer, A., Zachariah, M.R., Tarlov, M.J., Etzel, M., Brorson, K., The PDA Virus Filter Task Force, 2008. A consensus rating method for small virus-retentive filters. I. Method Development. PDA Journal of Pharmaceutical Science and Technology 62, 318–333.

Malloy, A., 2010. Characterizing Viral Titers in Manufacturing. Genetic Engineering and Biotechnology News. 30, 42–44.

Mulholland, G.W., Donnelly, M.K., Hagwood, C.R., Kukuck, S.R., Hackley, V.A., Pui, D.Y.H., 2006. Measurement of 100 nm and 60 nm particle standards by differential mobility analysis. J. Res. Natl. Inst. Stand. Technol. 111, 257–312.

Pease, L.F., Lipin, D.L., Tsai, D.H., Zachariah, M.R., Lua, L.H.L., Tarlov, M.J., Middleberg, A.P.J., 2009. Quantitative characterization of virus-like particles by assymetrical flow field fractionation, electrospray differential mobility analysis and transmission electron microscopy. Biotechnol. Bioeng. 102, 845–855.

Pease, L.F., Tsai, D.H., Brorson, K.A., Guha, S., Zachariah, M.R., Tarlov, M.J., 2011. Rapid physical characterization of icosahedral virus ultrastructure, stability and integrity using electrospray differential mobility analysis. Anal. Chem. 83, 1753–1759.

Pease, L.F., Tsai, D.H., Hertz, J.L., Zachariah, M.R., Tarlov, M.J., 2010. Packing and size determination of colloidal nanoclusters. Langmuir 26, 11384–11390.

Siuzdak, G., Bothner, B., Yeager, M., Brugidou, C., Fauquet, C.M., Hoey, K., Chang, C.M., 1996. Mass spectrometry and viral analysis. Chem. Biol. 3, 45–48.

Thomas, J.J., Bothner, B., Traina, J., Benner, W.H., Siuzdak, G., 2004. Electrospray ion mobility spectrometry of intact viruses. Spectroscopy 18, 31–36.

Tito, M.A., Tars, K., Valegard, K., Hajdu, J., Robinson, C.V., 2000. Electrospray time-of-flight mass spectrometry of the intact MS2 virus capsid. J. Am. Chem. Soc. 122, 3550–3551.

Tsai, D.H., Pease, L.F., Zangmeister, R.A., Tarlov, M.J., Zachariah, M.R., 2009. Aggregation kinetics of colloidal particles measured by gas-phase differential mobility analysis. Langmuir 25, 140–146.

Tsai, D.H., Zangmeister, R.A., Pease, L.F., Tarlov, M.J., Zachariah, M.R., 2008. Gas-phase ion-mobility characterization of SAM-functionalized Au nanoparticles. Langmuir 24, 8483–8490.

Wang, S.C., Flagan, R.C., 1990. Scanning electrical mobility spectrometer. Aerosol Science and Technology. 13, 230–240.

Weidensohler, A., 1988. An approximation of the bipolar charge distribution for particles in the submicron size range. J. Aerosol Sci. 19, 387–389.
Wick, C.H., Elashvili, I., Stanford, M.F., McCubbin, P.E., Deshpande, S.V., Kuzmanovic, D., Jabbour, R.E., 2007. Mass spectrometry and integrated virus detection system characterization of MS2 bacteriophage. Toxicol. Mech. Method 17, 241–254.
Xu, Y., Brorson, K., 2001. An overview of quantitative PCR assays for biologicals: quality and safety evaluation. Dev. Biol. (Basel) 113, 89–98.
Yao, Z.P., Demirev, P.A., Fenselau, C., 2002. Mass spectrometry-based proteolytic mapping for rapid virus identification. Anal. Chem. 74, 2529–2534.